Optical Materials 64 (2017) 64–69

Contents lists available at ScienceDirect

Optical Materials

journal homepage: www.elsevier.com/locate/optmat

Passive Q-switching of a Tm:YLF laser with a Co^{2+} doped silver halide saturable absorber

Harel Hecht [a, b], Zeev Burshtein [c], Abraham Katzir [d], Salman Noach [e], Maxim Sokol [c], Eugene Frumker [b], Ehud Galun [f], Amiel A. Ishaaya [a, *]

[a] Department of Electrical & Computer Engineering, Ben-Gurion University of the Negev, Beer-Sheva, 84105, Israel
[b] Department of Physics, Ben-Gurion University of the Negev, Beer-Sheva, 84105, Israel
[c] Department of Materials Engineering, Ben-Gurion University of the Negev, Beer-Sheva, 84105, Israel
[d] Department of Physics, Tel-Aviv University, Tel-Aviv, 6996801, Israel
[e] Department of Applied Physics, Jerusalem College of Technology, Jerusalem, 91160, Israel
[f] DDR&D, Ministry of Defense, Israel

ARTICLE INFO

Article history:
Received 12 September 2016
Received in revised form
25 October 2016
Accepted 13 November 2016

Keywords:
Solid-state lasers
Passive Q-switch
Laser materials
Silver halide

ABSTRACT

We report a successful passive Q-switching of a Tm:YLF laser operating at λ = 1.9 μm, using a Co^{2+}:$AgCl_{0.5}Br_{0.5}$ saturable absorber. Approximately 200-ns long, 150 μJ pulses were obtained. Increase in pump energy resulted in repetitive pulsing, with a repetition rate approximately proportional to the pump pulse energy. Room-temperature optical transmission saturation curves measured in ~1-mm thick Co^{2+}:$AgCl_{0.5}Br_{0.5}$ plates yielded a ground state absorption cross section $\sigma_{gs} = (7.8\pm0.5) \times 10^{-18}\ cm^2$, and an excited state absorption cross section $\sigma_{es} = (3.3\pm0.3) \times 10^{-18}\ cm^2$, at λ = 1.9 μm. The lifetime of the $A_2(^4F)$ second excited-state of the octahedral *O* symmetry was $\tau^* = (0.6\pm0.06)$ *ns*.

1. Introduction

1.1. Motivation

In the past two decades, many types of passive laser Q-switching materials were developed, the most popular were based on transition-metal cations like Cr^{4+}, Cr^{2+}, V^{3+}, or Co^{2+} as the active dopant [1–7]. For some important infrared lasers in the 1.3–1.7 μm range, especially for those exploiting the $^3I_{13/2} \rightarrow {}^4I_{15/2}$ emission of Er^{3+} ions, passive Co^{2+}:$Mg(Zn)Al_2O_4$ Q-switches represent an efficient solution [8–17]. Still, the $Mg(Zn)Al_2O_4$ Co^{2+} host production, even in the sintered polycrystalline (ceramic) phase, requires temperatures exceeding ~1500 °C [18]. Silver halide $AgCl_xBr_{1-x}$ crystals with 0 < x < 1, on the other hand, melt between 432 and 455 °C. Their single-crystal growth from melt is thus rather easy. Spectral applicability of Co^{2+} dopant ions for passive Q-switching may shift by using different hosts. Particularly, A Broad absorption band was observed in Co^{2+}-doped $AgCl_xBr_{1-x}$ crystals between ~1.5 and 2.3 μm [19], rendering this spectral region applicable for passive Q-switching. Furthermore, the crystals for all those compositions are transparent between 0.4 and 30 μm, with a refractive index of 2.0 < n < 2.2. These properties suggest their use in a variety of applications in the said, exceptionally broad, spectral range.

In this work we investigate a Co^{2+} doped silver halide $AgCl_{0.5}Br_{0.5}$ crystal as a passive Q-switch at the 1.885 μm wavelength. We performed optical bleaching experiments at 1.885 μm, and calculated various material parameters such as ground and excited-state absorption cross-sections, dopant densities, damage threshold, and the higher excited state lifetime. We demonstrate with this crystal, for the first time to the best of our knowledge, passive Q-switching inside a Tm:YLF laser oscillator [20] operating at λ = 1.885 μm.

1.2. Spectroscopic overview

Basically, the $AgCl_{0.5}Br_{0.5}$ composition forms a disordered crystal, related to the AgCl and AgBr parents. The latter each is face-centered cubic, belonging to the #225, $O_h^5(F4/m\bar{3}2/c)$ space

* Corresponding author.
E-mail address: ishaaya@ee.bgu.ac.il (A.A. Ishaaya).

http://dx.doi.org/10.1016/j.optmat.2016.11.022
0925-3467/

group. The (centered) unit cell contains 4 formula units. The Ag^+ ions occupy the 4a Wyckoff site of an octahedral O_h symmetry; the halogen singly negative ions occupy the 4b Wyckoff site of an octahedral O_h symmetry. The lattice parameters are 5.55 and 5.77 Å [21] for AgCl and AgBr, respectively. The $AgCl_{0.5}Br_{0.5}$ crystal exhibits similar features, except for disorder in the halogen sites, which may occupy either a chlorine or a bromine ion at 50% probability. The Ag^+ ion still maintains its octahedral coordination, yet at a reduced symmetry; an *O* symmetry may be considered a fair approximation. When doped to form a Co^{2+}:$AgCl_{0.5}Br_{0.5}$ crystal, the Co^{2+} ions replace two lattice Ag^+ ions, causing further distortion of the occupying sites. Spectroscopic studies indicate [22,23], that the majority of Co^{2+} ions are octahedrally coordinated, with six halogen nearest-neighbors. A smaller portion are tetrahedrally coordinated, with four halogen nearest neighbors. For spectroscopic analyses, those different sites may be approximated as having *O* and T_d symmetries, respectively. All optical transitions in the near, and mid-IR, the region of interest in our present study, relate to the crystal field splitting of the ^{4}F state Term of the free Co^{2+} ion. A variety of optical properties were measured in Co^{2+}:$AgCl_{0.5}Br_{0.5}$ between 300 and 20 K. A Broad absorption band was observed between ~1.5 and 2.3 μm [19], in addition to three bands around 0.64, 0.9, and 4.25 μm. The emission lifetime of the ~4.4 μm-centered band under excitation at 1.92 μm, varied between 1.73 ms at low temperatures, and 5 μs at room temperature [24].

A Co^{2+}:$AgCl_{0.5}Br_{0.5}$ energy level diagram relevant to the said prospected application is provided in Fig. 1. The two types of possible cobalt centers, octahedral and tetrahedral [19,22–24], are addressed. In the octahedral *O* crystal field symmetry, the ^{4}F state splits into $T_1(^4F) + T_2(^4F) + A_2(^4F)$ in an increasing energy order. Each state is further split by the smaller spin-orbit interaction, according to $^4F_{9/2} + {}^4F_{7/2} + {}^4F_{5/2} + {}^4F_{3/2}$ in an increasing energy order. $T_1(^4F_{9/2})$ is thus the ground state.

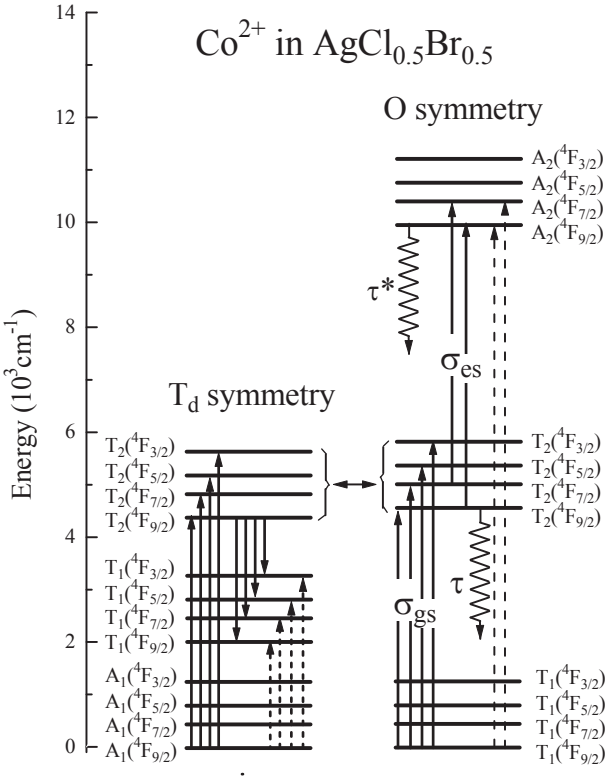

Fig. 1. Co^{2+}:$AgCl_{0.5}Br_{0.5}$ energy level diagram relevant for its function as a saturable absorber. The peak absorption wavelength of the $\boldsymbol{T_1(^4F)\rightarrow T_2(^4F)}$ transition in the octahedral site, and $\boldsymbol{A_1(^4F)\rightarrow T_2(^4F)}$ transition in the tetrahedral site, is around λ = 1.9 μm [23]. For details, see text.

The spin-orbit split states energies follow the well-known relation

$$\Gamma_{SLJ} = \tfrac{1}{2}\xi_{SL}[J(J+1) - L(L+1) - S(S+1)], \quad (1)$$

where $\boldsymbol{\Gamma_{SLJ}}$ is the level splitting, $\boldsymbol{\xi_{SL}}$ is the spin-orbit coupling coefficient, and L, S, and J are the orbital, spin, and total angular momentum numbers, respectively. The value $\boldsymbol{\xi_{SL} \cong -100 cm^{-1}}$ was assumed schematically for both *O* and T_d sites. In The *O* symmetry, $T_1(^4F)\rightarrow T_2(^4F)$ and $T_2(^4F)\rightarrow A_2(^4F)$ transitions are electric-dipole allowed. Such transitions are marked in the figure by solid arrows. The $T_1(^4F)\rightarrow A_2(^4F)$ transitions are electric-dipole forbidden; they are thus very weak, and marked by dashed arrows. The $T_1(^4F)\rightarrow T_2(^4F)$ transitions relate to the present, saturable ground-state absorption study at 1.9 μm; their cross section is thus marked σ_{gs}, and the excited $T_2(^4F)$-state lifetime is marked τ. The $T_2(^4F)\rightarrow A_2(^4F)$ transitions relate to the present, excited-state absorption study at 1.9 μm; their cross section is thus marked σ_{es}, and the higher excited $A_2(^4F)$ state lifetime is marked τ*. It is assumed (and proven in our present study) that $\tau^* \ll \tau$.

In the tetrahedral T_d crystal field symmetry, the ^4F state splits into $A_1(^4F) + T_1(^4F) + T_2(^4F)$ in an increasing energy order. Each state is further split by the smaller spin-orbit interaction, same as in the octahedral site. $A_1(^4F_{9/2})$ is thus the ground state, assumed to coincide with the O-symmetry one. The $A_1(^4F)\rightarrow T_2(^4F)$ and $T_2(^4F)\leftrightarrow T_1(^4F)$ transitions are electric-dipole allowed. Such transitions are marked in the figure by solid arrows. The $A_1(^4F)\leftrightarrow T_1(^4F)$ transitions are electric-dipole forbidden; they are thus very weak, and marked by dashed arrows. The $T_2(^4F)\rightarrow T_1(^4F)$ decay transitions relate to the Co^{2+} measured fluorescence at ~4.4 μm [19]. The absorption spectra in the vicinity of 1.9 μm involve excitation of Co^{2+} in both octahedral and tetrahedral sites; energy exchanges between the excited two type sites are also likely to occur.

Notably, Washimiya [22] erroneously presented a different assignment for the tetrahedral T_d crystal-field splitting of Co^{2+} ions ^{4}F-states in KCl crystal (specifically, $A_2(^4F) + T_2(^4F) + T_1(^4F)$ in an increasing energy order). Their optical transitions assignments are correspondingly erroneous. This error has permeated into virtually all later publications by others, such as in Refs. [17,23–26].

1.3. Experimental setup and procedure

Bridgman-Stockbarger grown Co^{2+}:$AgCl_{0.5}Br_{0.5}$ crystalline cylindrical boules [24], ~7-cm long and approximately 8–10 mm in diameter, were used as starting material. Discs, ~1–3.5 mm thick, were cut and optically polished. To prevent bending during cutting, the sample was side mounted to an aluminium rod using bee wax. Cutting was done under a minimal load at a moderate speed of 250 rpm using a tabletop precision cut-off machine (Minitom by Struers ApS). The 0.15 mm thick cutting wheel was a low-concentration diamond-metal bonded (Struers ApS). Dual side plane grinding to the desired thickness was done sequentially from coarse (SiC grinding paper, 220 grit) to fine (SiC grinding paper, 4000 grit) using a grinding and polishing machine (LaboSystem Struers ApS) under a 10 N load at 150 rpm. Residual surface damage was removed by additional polishing by 3 and 1 μm diamond powder suspensions (DiaPro Dac 3-μm/1-μm by Struers ApS) on a 20-cm aluminium wheel topped with a woven acetate fabric (MD-Dac, Struers ApS) at 5 N load. Final polishing was done by a 0.25 μm diamond powder suspension using a woven silk fabric (MD-Dur,